Volume 3
Number 2
March 2025
Pages 345–640

Sustainable Food Technology

rsc.li/susfoodtech

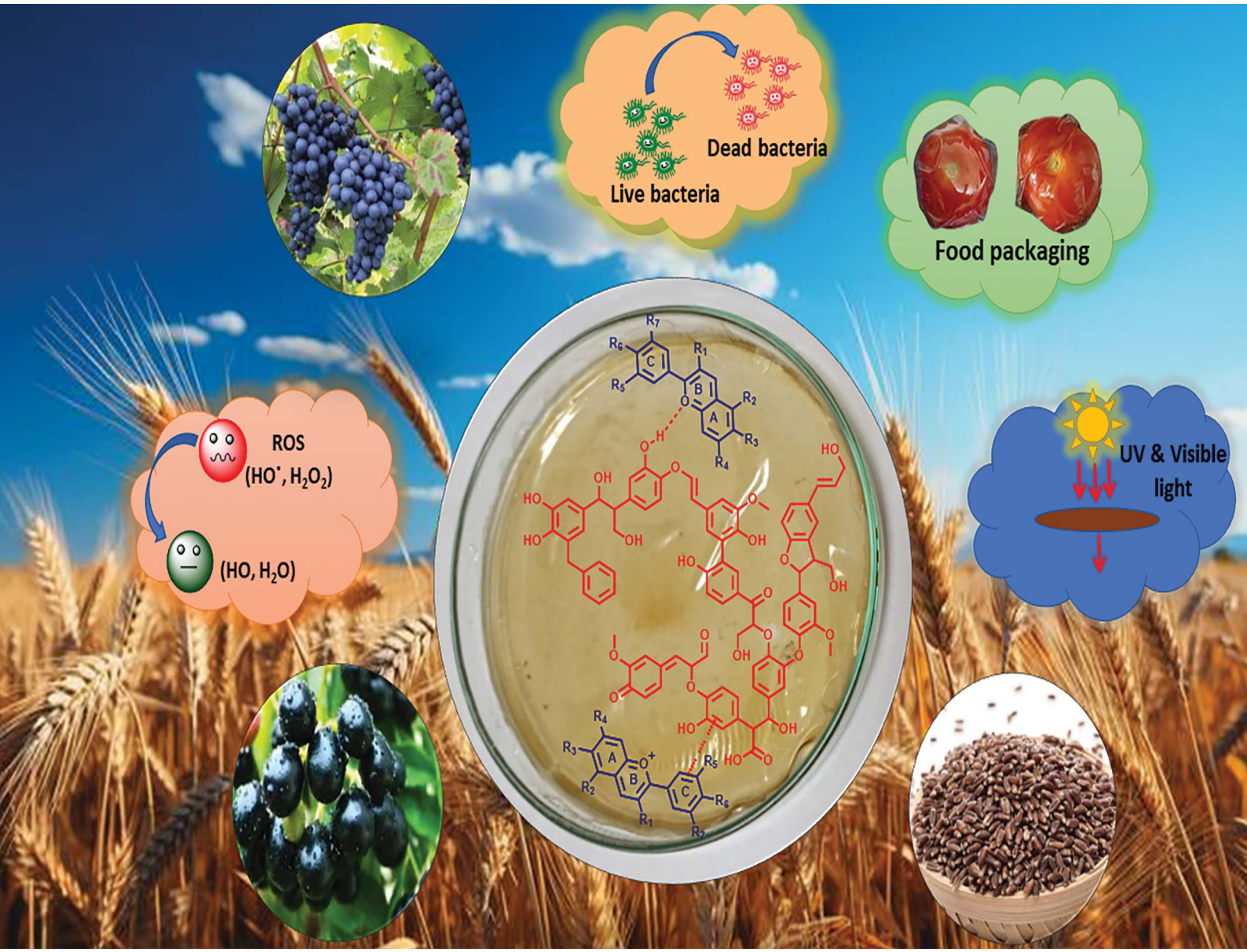

ISSN 2753-8095

ROYAL SOCIETY OF CHEMISTRY

PAPER

Jayeeta Bhaumik, Maninder Meenu, and Monika Garg *et al.*
Development of bionanocomposite packaging films based on lignin nanoencapsulated anthocyanins extracted from agro-waste for enhancing the post-harvest shelf life of tomatoes

Sustainable Food Technology

ROYAL SOCIETY OF CHEMISTRY

PAPER

View Article Online
View Journal | View Issue

Cite this: *Sustainable Food Technol.*, 2025, **3**, 414

Development of bionanocomposite packaging films based on lignin nanoencapsulated anthocyanins extracted from agro-waste for enhancing the post-harvest shelf life of tomatoes†

Maninder Meenu,*[a] Anil Kumar Pujari,[b] Seema Kirar,[b] Mansi,[b] Aniket Thakur,[b] Monika Garg [a] and Jayeeta Bhaumik [b]

Anthocyanin, a natural pigment from the flavonoid family, can be useful as a natural colorant in the packaging industry. Due to the sensitivity to light, pH and temperature of anthocyanin, its applications are restricted. In the present study, anthocyanins extracted from black wheat bran (WB), black plum (BP) and blueberry (BB) were nanoencapsulated using a natural biopolymer, lignin, to enhance stability and improve the biological properties of anthocyanins. The synthesized nanoparticles (A-LNPs) exhibited satisfactory encapsulation efficiency (92.32 to 72.26%), size (126.13 to 145.17 nm), PDI (0.140 to 0.172), and zeta potential (−36.27 to −34.10 mV), and potent antioxidant and antibacterial activity against *Staphylococcus aureus*. These novel A-LNPs were observed to be light stable during 28 days of storage at room temperature compared to purified anthocyanins. A-LNPs were further used as active ingredients to develop polyvinyl alcohol–polyethylene glycol (PVA–PEG)-based packaging films. These PVA–PEG-A-LNP films were observed to retain the quality parameters of tomatoes for at least 15 days of storage compared to tomatoes packed with PVA–PEG films and control samples. Such biocompatible packaging films can serve as alternative materials to conventional plastic.

Received 15th November 2024
Accepted 13th February 2025

DOI: 10.1039/d4fb00342j

rsc.li/susfoodtech

Sustainability spotlight

In the present study, anthocyanins were extracted from agro-waste, purified, and then nanoencapsulated using lignin (A-LNPs). The encapsulation of anthocyanin using lignin leads to enhanced stability, antioxidant activity, and antimicrobial activity of A-LNPs compared to purified anthocyanins and lignin. Overall, BB resulted in the highest TAC (194.45 mg per kg WB) and good encapsulation efficiency (92.32%) along with potent antioxidant (73.32–79.56%) and antibacterial activity (15.82 μg mL^{-1}) against *S. aureus*. Furthermore, 15% BB@ALNPs was used as an active ingredient for developing PVA–PEG-based packaging films. These films exhibited excellent tensile strength, UV-blocking, and fluorescence properties. These films were also characterized by employing SEM and FTIR spectroscopy. Furthermore, tomatoes were packaged with PVA–PEG_15%BB@ALNPs and PVA–PEG-based films. The samples packaged with PVA–PEG_15%BB@ALNPs films presented high resistance towards quality deterioration compared to tomatoes packaged with PVA–PEG films and control samples during 15 days of storage at room temperature. In the future, the antimicrobial potential of PVA–PEG_15%BB@ALNPs films can be explored against various food-borne pathogens. In addition, PVA–PEG_15%BB@ALNPs films can also be employed as an intelligent packaging or biosensor to monitor the shelf life of various perishable food products based on the fluorescence properties of PVA–PEG_15%BB@ALNPs films. Overall, the present findings will contribute significantly towards the sustainable development goals set by the United Nations and the Government of India's vision to be among the top five global biomanufacturing hubs by 2025.

Introduction

Anthocyanins are well-known bioactive compounds associated with the flavonoid family. Anthocyanins are responsible for various colors observed in various fruits, vegetables, flowers, and cereal crops. Structurally, these water-soluble pigments are glycosylated anthocyanidins and share diphenylpropane skeletons ($C_6C_3C_6$).[1,2] There are approximately more than 700 distinct types of anthocyanins observed in nature. Among them, cyanidin, delphinidin, pelargonidin, malvidin, peonidin, petunidin and their methylated derivatives namely, malvidin, peonidin,

[a]*Division of Agricultural Biotechnology, National Agri-Food Biotechnology Institute (NABI), Sector 81, Sahibzada Ajit Singh Nagar, Punjab-140308, India. E-mail: meenu_maninder@yahoo.com; mkajgarg@gmail.com; Tel: +91 7589592370; +91 1725221205*

[b]*Department of Nanomaterial and Application Technology, Center of Innovative and Applied Bioprocessing (CIAB), Sector 81, Sahibzada Ajit Singh Nagar, Punjab-140308, India. E-mail: jayeeta@ciab.res.in; Tel: +91 1725221539*

† Electronic supplementary information (ESI) available. See DOI: https://doi.org/10.1039/d4fb00342j

and petunidin are the most common anthocyanins.[1,3] Glucose, arabinose, galactose, xylose, and sambubioside are the most common sugars bound to anthocyanidins to form anthocyanins. Anthocyanins are frequently employed as natural substitutes for synthetic colors in food, cosmetics, and pharmaceutical industries.[2,4,5] In addition to their attractive hues, anthocyanins are also recognized for their profound biological activities, which include antimicrobial, antioxidant, neuroprotective, anti-inflammatory, anti-obesity, anti-diabetic, anti-carcinogenic, and cardioprotective effects.[2,6] Among the polyphenols, anthocyanins are widely used additives to develop smart packaging due to their non-toxic, eco-friendly nature and affordability.[4] Anthocyanin-enriched packaging films exhibit potent antibacterial and antioxidant effects. This in turn, extends the shelf life, retains nutritional value, and maintains the overall quality of a variety of food products.[4,7]

However, the application of anthocyanins in food, pharma, and cosmetic industries is challenging due to the poor stability and susceptibility to degradation due to high pH, light, and temperature.[2,5] Thus, to deal with this issue, researchers are extensively exploring nanoencapsulation of anthocyanins using various wall materials such as polysaccharides, proteins, and lipids to improve stability, bioavailability, and controlled release.[3,5]

Previously, anthocyanins from *Ardisia compressa* seeds, raspberry pomace, standard anthocyanin (Cyanidin 3-*O*-glucoside), blackberry, pomegranate peel extract, and mulberry were encapsulated using corn starch,[8] amphiphilic peptide,[9] pectin–lysozyme self-assembly,[10] maltodextrin, whey protein isolate,[11] and caseinate–konjac glucomannan,[6] respectively. Lignin is another frequently employed wall material for nanoencapsulation of various bioactive compounds such as curcumin,[12] essential oils,[13] naringin,[14] beta-carotene,[15] and pyranoanthocyanin pigments.[16] Lignin is the second most abundant plant-based under-utilized polymer in nature after cellulose. Lignin also exhibits significant antioxidant and antimicrobial properties attributed to its various polyphenolic groups.[17–19] All these properties make lignin a suitable wall material for nanoencapsulation of anthocyanin.

Thus, in the present study, anthocyanins extracted from black wheat bran (WB), poor-graded black plum (BP), and blueberry (BB) were used. Furthermore, isolated anthocyanins were characterized and encapsulated using kraft lignin. Furthermore, the stability, antioxidant activity, and antimicrobial activity of these anthocyanin lignin nanoparticles (A-LNPs) were explored. These novel A-LNPs were further used to develop active packaging films, and the capability of these films to enhance the shelf life of tomatoes was also explored. This natural pigment-based green packaging material can be a biosafe replacement for existing chemical-based plastics.

Experimental section

Materials

All the chemicals used in this study were of analytical grade and procured from Central Drug House (P) Ltd – CDH, New Delhi, Sisco Research Laboratories Pvt. Ltd (SRL), Mumbai, India, and Sigma-Aldrich, India. Tryptone soya broth and agar were purchased from HiMedia, India. Ultrapure water was collected from a Direct-Q®3 UV water purification system provided by Merck Millipore, Mumbai, India. *Staphylococcus aureus* (MTCC 1430) was obtained from the Microbial Type Culture Collection and Gene Bank (MTCC), Chandigarh, India.

Raw material for anthocyanin

Black wheat (NABI MG-11) bran (WB) was the by-product of bakery experiments conducted at NABI Mohali. For poor-graded black plum (BP), over-ripened fruit drops were collected from NIPER Mohali. Wrinkled and shrivelled blueberries (BB) were collected from the local market of Chandigarh. All the samples were collected in the year 2023. Fruit samples were cleaned to remove any foreign material and bruised fruit and then washed under running tap water. After washing, the samples were air-dried, and BP was deseeded, and then all samples were processed to make a paste using a blender. All the samples were stored at −80 °C in air-tight food-grade containers until further analysis.

Anthocyanin extraction and purification

Anthocyanins were extracted from WB using conventional shaking according to a previously reported method[20] with slight modifications. Briefly, 100 g of the sample was mixed with 1 L acidic water containing 1% HCl (v/v) followed by shaking at 120 rpm in the dark for 18 hours at 28 °C. The resultant mixture was centrifuged at 10 000 rpm for 20 min at 4 °C to collect the supernatant using a centrifuge (5415 R, Eppendorf, Germany). Again 1 L of solvent was added to the pellet and the mixture was shaken for 5 h, followed by centrifugation to collect the supernatant. Both supernatants were combined and kept overnight at −20 °C for precipitation of heavier molecules followed by centrifugation to collect the clear supernatant, and then the samples were lyophilized.

Ultrasonic-assisted extraction (UAE) was conducted to extract anthocyanin from BP and BB by employing the previously described method[21] with slight modifications. Briefly, a 100 g sample (BP, BB) was mixed with 1 L aqueous acidic ethanol (72.5% EtOH and 0.02% HCl v/v) and UAE was carried out twice for 30 minutes at 40 kHz and 480 W using an ultrasonicator (Branson M2800H-E, Danbury, USA) followed by centrifugation by employing other steps as mentioned in the case of WB to achieve lyophilized anthocyanin extract.

Furthermore, lyophilized anthocyanin extracts from WB, BB, and BP were purified by employing ion exchange chromatography with Amberlite XAD-7 as the resin according to a previously reported method.[22] The resultant purified anthocyanin extract was concentrated using a rotary evaporator and then lyophilized and stored at −80 °C.

Determination of total anthocyanin content

The total anthocyanin content of the samples was determined using a previously reported method.[20] The absorbance of purified anthocyanin extract was observed at 525 nm using a UV-vis spectrophotometer (UV-2600, Shimadzu, India). Concentration

of total anthocyanin in the extract was expressed as milligrams (mg) of cyanidin 3-glucoside equivalents per kilogram (kg) of samples.

$$C = (A/e) \times (V/1000) \times M_W \times (1/\text{sample weight}) \times 10^6$$

where C is the concentration of total anthocyanin (mg kg^{-1}), A is the absorbance of the extract, e is the molar absorptivity of cyanidin 3-glucoside (25 965 cm^{-1} M^{-1}), V is the total volume of anthocyanin extract used, and M_W is the molecular weight of cyanidin 3-glucoside.

Nanoencapsulation of purified anthocyanins using lignin

A-LNPs were synthesized by employing the green solvent–anti-solvent method using ethanol and water according to a previously reported method[17] with slight modifications. Briefly, kraft lignin (10 mg) and anthocyanin (1 mg) were dissolved in ethanol (1 mL). This solution was added dropwise in deionized water (10 mL) under sonication at 40 kHz and 480 W for 10 min. The ratio of lignin and anthocyanin (10 : 1, 10 : 3, 10 : 5, and 10 : 10 w/w) in the reaction mixture was optimized based on the Dynamic Light Scattering (DLS) data of the resultant A-LNPs. Furthermore, ethanol was removed under reduced pressure. The remaining solution was centrifuged at 14 000 rpm for 10 minutes at 4 °C. The obtained pellet was resuspended in water for lyophilization and then characterized by employing various analytical techniques.

Characterization of anthocyanin-loaded lignin nanoparticles (A-LNPs)

Dynamic light scattering analysis. The size, PDI, and zeta potential of bare LNPs and A-LNPs were analyzed using dynamic light scattering equipment (Nano-ZS, Malvern, India) at 25 °C with a fixed angle detector 173°. For this, a diluted sample (1 : 100 v/v) of synthesized LNPs and A-LNPs in distilled water was taken.[10]

Encapsulation efficiency. The encapsulation efficiency of the synthesized A-LNPs was determined using a previously reported method.[9] The synthesized A-LNPs were centrifuged at 14 000 rpm for 10 min at 4 °C to separate the encapsulated nanoparticles from the solution. The absorbance of the supernatant was observed at 525 nm to determine the concentration of free anthocyanins by comparing it with the calibration curve developed using purified anthocyanins (5–50 μg mL^{-1}).

Morphological characterization. The bare LNPs and A-LNPs were drop cast on silicon wafers, and dried overnight. Then, these dried samples were gold coated with an ion sputtering system (Q150T ES Quorum, UK) for 2 min and observed under a scanning electron microscope (1142265, Thermo Fisher, Czech Republic) at 10 kV. HR-TEM analysis of bare LNPs and L-ANPs was conducted using a TEM instrument (FEI Tecnai G2, Helmholtz Imaging, Germany) at NIPER, Mohali.

Fourier-transform infrared (FTIR) spectroscopy. The FTIR spectra of kraft lignin, bare LNPs, purified anthocyanins, and lyophilized L-ANPs were recorded with an FTIR spectrometer (UATR Two, PerkinElmer, USA) equipped with an attenuated total reflectance (ATR) accessory. The sample was placed on a diamond crystal, and spectra were collected from 4000 to 400 cm^{-1} with a spectral resolution of 4 cm^{-1} while keeping the sample in contact with the diamond crystal.

Stability study of anthocyanin-encapsulated lignin nanoparticles

The bare LNPs and A-LNPs were stored at room temperature. The samples were exposed for 28 days to natural light daily for up to 16 h. The DLS data of A-LNPs diluted with distilled water (1 : 100 v/v) were collected at an interval of one week using dynamic light scattering equipment at 25 °C with a fixed angle detector of 173°.

Antioxidant and antibacterial activity of A-LNPs

The antioxidant activity of purified and encapsulated anthocyanins was explored by employing DPPH and ABTS assay[17,18] as mentioned in the literature. Briefly,7 mM ABTS solution was added to 2.45 mM potassium persulphate (1 : 1, v/v) to prepare ABTS free radical solution. This solution was incubated for 12 h in the dark at room temperature to complete the reaction and achieve stabilized absorbance. Then 140 μL ABTS free radical solution was mixed with 850 μL A-LNPs, followed by vigorous shaking. Then, the reaction mixture was incubated for 15 min at room temperature. The absorbance of the resultant reaction mixture was observed at 734 nm. The percentage scavenging activity of ABTS free radicals by A-LNPs was calculated using the following equation:[17]

$$\text{ABTS scavenging activity (\%)} = (\text{Abs}_{\text{control}} - \text{Abs}_{\text{sample}})/\text{Abs}_{\text{control}} \times 100$$

where $\text{Abs}_{\text{control}}$ is the absorbance of ABTS cation radical solution, and $\text{Abs}_{\text{sample}}$ is the absorbance of ABTS cation radical solution after reaction with A-LNPs.

For DPPH assay, 0.14 mM DPPH solution was prepared in methanol. A-LNPs (50 μg mL^{-1}) were prepared in a mixture of methanol and ethanol (1 : 1 v/v). Then, 850 μL A-LNPs was added to 140 μL DPPH solution followed by vigorous shaking. The resultant reaction mixture was incubated in the dark at 37 °C. After 30 min, the absorbance of the reaction mixture was recorded at 517 nm. The percentage scavenging activity of DPPH free radicals by A-LNPs was calculated using the following equation:[18]

$$\text{DPPH scavenging activity (\%)} = (\text{Abs}_{\text{control}} - \text{Abs}_{\text{sample}})/\text{Abs}_{\text{control}} \times 100$$

where $\text{Abs}_{\text{control}}$ is the absorbance of only the DPPH solution and $\text{Abs}_{\text{sample}}$ is the absorbance of the DPPH cation radical after reaction with A-LNPs.

The antimicrobial activity of purified anthocyanins and encapsulated anthocyanins was explored against the most prevalent food-borne pathogen *S. aureus*.[18] Briefly, the *S. aureus* (OD = 0.6) was treated with different concentrations (0–120 μg mL^{-1}) of purified anthocyanins and A-LNPs and incubated at 37 °C for 6 h. The treated bacterial cells were spread on media

plates, and the number of colonies (CFU mL^{-1}) was counted after 24 h of incubation. The growth of treated microbial cells was compared with control plates to assess the antimicrobial activity of different samples. The IC_{50} value of purified anthocyanins and A-LNPs was calculated using a standard linear calibration equation at 0–120 μg mL^{-1}.

Preparation of polyvinyl alcohol–polyethylene glycol (PVA–PEG)-A-LNPs packaging films

A previously reported casting method was used to prepare PVA–PEG-based packaging films.[19] For the same, 300 mg of PVA powder was mixed in 30 mL of distilled water and heated at 80 °C for 30 min, followed by the addition of 300 mg of PEG-400. After 15 min of stirring, A-LNPs were added at optimal concentrations (15% w/w) and stirred for 1 h. The resultant solution was cast into Petri plates and dried at 45 °C. After 12 h of drying, PVA–PEG-A-LNPs films were removed from the Petri plates and used for further analysis.

Characterization of PVA–PEG-A-LNPs packaging films

The characterization of bare PVA–PEG and PVA–PEG-A-LNPs-based packaging films included measurement of thickness, SEM, UV and FTIR spectrum recorded according to previously reported methods as described in section S1.1–S1.4.†[19] Briefly, the thickness of bare PVA–PEG and PVA–PEG-A-LNPs films was determined using a digital micrometer (IP65, Mitutoyo, Brazil) as mentioned in the literature. The morphology of films was observed under a scanning electron microscope as mentioned earlier and the FTIR spectra of bare PVA–PEG and PVA–PEG-A-LNPs films was acquired as described earlier. The UV-vis spectra of bare PVA–PEG and PVA–PEG-A-LNPs films were acquired by employing a UV-vis spectrophotometer. The fluorescence behaviour of the PVA–PEG-A-LNPs film was explored by exposing films to UV light at 365 nm (254/365 nm, Analytik, USA). The tensile strength and elongation at break of packaging materials were calculated using data from acquired a Texture Analyser (TA-HD plus, Stable Micro Systems, UK) equipped with a 50 kN load cell equipped with tensile grips as described in section S1.5–S1.6.†[19] The water vapour transmission rate (WVTR) was also determined according to the method mentioned in section S1.6.†[23] Additionally, the migration test of packaging films was performed using water, 3% acetic acid (w/v), and 50% ethanol (v/v) as aqueous simulants according to a previously described method (refer to S1.7†).[23,24]

Impact of the PVA–PEG-A-LNPs film on the shelf-life of tomatoes

Fresh and clean tomatoes ($n = 180$) of the same maturity level, size, and shape were randomly divided into three groups. One group was considered as a control group and the other groups were packaged with PVA–PEG and PVA–PEG-A-LNPs films. Another 30 tomato samples were divided into three groups to observe changes in color and weight loss during storage. All samples were stored at room temperature for 15 days. The quality analysis of tomatoes was conducted on day 0, day 3, day 6, day 9, day 12, and day 15 as described in the literature.[25]

Quality analysis of tomatoes. The firmness of tomatoes was measured using a Texture Analyser (TA-HD plus, Stable Micro Systems, UK) as mentioned in ESI S2.1,† and the color of the samples was measured using a colorimeter (CR 400, Konica Minolta, Japan) as discussed in section S2.2 of ESI.† The weight loss, pH, total soluble solids, and titratable acidity of tomatoes were measured according to methods mentioned in ESI S2.3–S2.6.†[25]

Statistical analysis

Each experiment was conducted in triplicate and data were presented as mean ± standard deviation. Statistical analysis was conducted by employing one-way ANOVA using SPSS ver. 19 (IBM, USA). Graphs were plotted using Origin 2021 software (OriginLab Co. Ltd, USA). The $p \leq 0.05$ presented significant differences among the mean values of different samples.

Results and discussion

Anthocyanin extraction and purification

Anthocyanin extraction from WB was optimized using the conventional shaking method using acidic water at different time intervals. It was observed that conventional shaking for 6 + 5 h resulted in the highest anthocyanin extraction (210.11 mg per kg dry basis) compared to 30 min + 5 h, 1.5 + 5 h, and 3 + 5 h as mentioned in ESI Table 1.† Whereas, extraction for 18 + 5 h resulted in comparable anthocyanin extraction to that for 6 + 5 h. In the case of BP fruit drops and shrivelled BB, anthocyanin extraction was optimized using UAE at different time intervals. It was observed that UAE for 30 + 30 min resulted in the highest anthocyanin extraction in both BP (42.67 mg per kg wet basis) and BB (194.45 mg per kg wet basis). However, a significant decrease in TAC was observed in both fruits with an increase in the extraction time (ESI Table 1†). Similar results were also reported in a previous study where the TAC content of BB pomace was increased to 11.00 mg g^{-1} after 40 min UAE and then decreased with a further increase in the UAE time. It was mentioned that too long an extraction time may lead to structural destruction of anthocyanin which in turn reduces anthocyanin yield.[26] It is also interesting to note that conventional shaking with acidic water for 16 + 5 h resulted in poor anthocyanin extraction from BP and BB. These crude anthocyanin extracts of WB, BB, and BP were 95.98%, 95.82%, and 92.96% reduced compared to their original sample weight. After the removal of protein or any hydrocolloids present, the resultant semi-pure extracts were reduced by 40.30%, 40.67%, and 67.74% of crude extract weight in the case of WB, BB, and BP, respectively. These extracts were further purified using Amberlite XAD-7 resin and the resultant purified anthocyanin extracts were reduced to 92.75%, 96.61%, and 95.83% compared to semi-pure anthocyanin extracts of WB, BB, and BP, respectively. These observations are in accordance with a previous study that purified anthocyanins from edible flowers.[22]

Optimization of the lignin-to-anthocyanin ratio for synthesizing A-LNPs

During nanoencapsulation of the active material, nanoparticles with smaller size are preferred due to their higher stability;

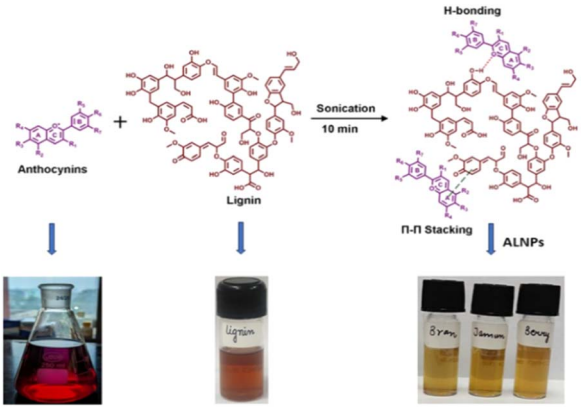

Scheme 1 Schematic presentation of synthesis of A-LNPs from anthocyanins and lignin using sonication as a top-down technique.

resistance towards precipitation, and enhanced functionality.[27] It was also reported that a higher quantity of wall material or core material resulted in an increased size of the resultant nanoparticles.[28] Thus, optimizing the quantity of the wall material and core material to synthesize highly stable nanoparticles with the smallest size is of immense importance. Furthermore, the purified anthocyanins were encapsulated using commercial kraft lignin as shown in Scheme 1. Initially, lignin-to-anthocyanin ratios (10 : 1, 10 : 3, 10 : 5, and 10 : 10 w/w) were optimized, and DLS data (size, PDI and zeta potential) of resultant nanoparticles were recorded. Interestingly, BP@ALNPs, WB@ALNPs, and BB@ALNPs showed particle sizes ranging from 133.53–154.40 nm, 126.13–154.97 nm, and 145.17–234.70 nm, respectively, whereas PDI varied from 0.140–0.157, 0.172–0.210, and 0.155–0.402, respectively. Furthermore, the zeta potential was recorded as −34.1 to −34.3, −36.27 to −33.23, and −36.10 to −31.93 mV, in the case of BP@ALNPs, WB@ALNPs, and BB@ALNPs, respectively. Zeta potential is a key parameter that governs the stability of nanoparticles through electrostatic repulsion. Nanoparticles with zeta potential values from +30 to −30 mV are considered stable colloids. As a result, these nanoparticles are less vulnerable to agglomeration and destabilization forces such as van der Waals forces, particle–particle interactions, and Brownian motion.[29] Conclusively, a lignin-to-anthocyanin (BP, WB, and BB) ratio of 10 : 1 (w/w) was selected for the development of A-LNPs for further studies as this particular concentration resulted in the best DLS data in terms of size, PDI, and zeta potential as shown in ESI Table 2.†

Encapsulation efficiency of anthocyanin-encapsulated lignin nanoparticles (A-LNPs). Furthermore, the encapsulation efficiency of synthesized A-LNPs was calculated. The highest encapsulation efficiency (92.32%) was observed in the case of BB@ALNPs, followed by BP@ALNPs (83.18%) and WB@ALNPs (72.41%) as mentioned in ESI Table 3.† Thus, it can be depicted that anthocyanins extracted from BB, BP, and WB were efficiently loaded on LNPs. These findings are in compared with previous reports where resveratrol and pyranoanthocyanin were encapsulated in lignin with >90% and 85–85% encapsulation efficiency.[30,31] The variation in the encapsulation efficiency of resultant A-LNPs depends on the interaction of kraft lignin and anthocyanins. Furthermore, the chemical composition of anthocyanin extract and low concentration also significantly impact encapsulation efficiency. Because different types of anthocyanins exhibit different polarities and solubilities,[2] the interaction of anthocyanin from various sources with lignin will be different. It is also important to consider that the degradation of anthocyanin in a raw material and during processing (extraction to purification) also alters the functional groups responsible for interaction with lignin which in turn affects the encapsulation efficiency of A-LNPs. Based on previous studies, malvidin 3-glucoside, delphinidin 3-glucoside, petunidin 3-glucoside and cyanidin 3-galactoside are the major compounds in BB.[32] In the case of BP, delphinidin 3,5-*O*-diglucoside, malvidin 3,5-*O*-diglucoside, and petunidin 3,5-*O*-diglucoside are the major anthocyanins.[33] Whereas, delphinidin-3-*o*-rutinoside, delphinidin-3-*o*-diglucoside, and delphinidin-3-*o*-galactoside are the major anthocyanins reported in black wheat (WB).[34] In addition, the quantity of individual anthocyanin may also vary depending on the cultivar, geographical location, and ripening or maturity stage of the plant material.[2] Thus, in the present study, variations in encapsulation efficiency may be attributed to the significant variation in composition and quantity of individual anthocyanins.

Characterization of A-LNPs. The particle size, PDI, and zeta potential of synthesized A-LNPs at an optimized lignin: anthocyanin concentration (10 : 1) were recorded using dynamic light scattering (DLS). As shown in ESI Fig. 1,† bare LNPs showed the least particle size of ∼119 nm, a PDI of 0.150, and a zeta potential of −36 mV. Notably, the size of BP@ALNPs was ∼133 nm with 0.135 PDI, and ∼−33 mV surface charge. The BB@ALNPs showed a particle size, PDI, and zeta potential of 146 nm, 0.160, and −36 mV, respectively. Moreover, the WB@ALNPs showed a particle size, PDI, and zeta potential of 125 nm, 0.167, and −36 mV, respectively. The increase in the particle size of synthesized A-LNPs indicates the encapsulation of anthocyanins inside LNPs. The insignificant change in the zeta potential of bare LNPs and A-LNPs represents an encapsulation of ACN in lignin that didn't change the surface charge of LNPs. Furthermore, the presence of a negative charge on the surface of A-LNPs results in repulsion between A-LNPs that contributes towards their stability.[30] Previously, a study where pyranoanthocyanin and resveratrol were entrapped in lignin nanoparticles also resulted in similar findings with a size of 150–250 nm, PDI <0.2, and a zeta potential of around −44 to −33.4 mV.[30,31]

Morphological analysis of the synthesized A-LNPs. Furthermore, the morphological characterization was performed using field emission-scanning electron microscopy (FE-SEM) of the synthesized nanoparticles at 500 nm (ESI Fig. 2†). The synthesized nanoparticles exhibited particle sizes of around 100–150 nm. Subsequently, the synthesized particles were spherical. Conclusively, the synthesized A-LNPs showed a small increment in their particle size (∼119 to ∼198 nm) compared to bare LNPs (∼61 to ∼93 nm), indicating encapsulation of anthocyanins in LNPs. Similar findings were also observed in the case

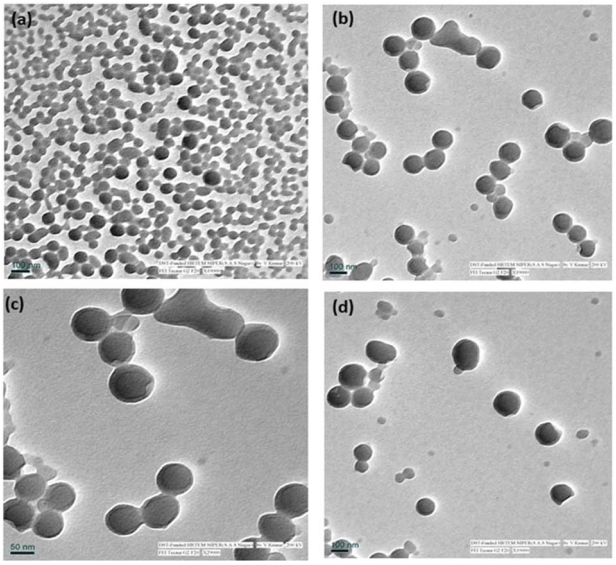

Fig. 1 TEM analysis of L-ANPs (a) bare LNPs, (b) BP@ALNPs, (c) BB@ALNPs, and (d) WB@ALNPs.

of TEM images as shown in Fig. 1. The synthesized bare LNPs and A-LNPs exhibited a symmetrical and spherical shape. Previous studies have also reported the formation of uniform spherical LNPs due to good lignin solubility in ethanol and poor solubility in water which leads to appropriate interactions between water and lignin during the nanoencapsulation process.[35] It was also observed that the inclusion of anthocyanins in LNPs did not change the shape of A-LNPs. Similar results were also reported in the case of bare LNPs, iron(III)-complexed LNPs, pyranoanthocyanin-LNPs, and resveratrol-LNPs.[30,35,36] Moreover, minor difference in DLS and electron microscopy results were observed. This may be attributed to the fact that DLS represents average hydrodynamic diameter of nanoparticles in entire sample, whereas electron microscopy represents actual size of nanoparticles in a small section of a sample.[35] In addition, a slight increase in the size of A-LNPs was also observed, indicating successful encapsulation of anthocyanins in LNPs.

Fourier-transform infrared (FTIR) spectral analysis of A-LNPs. The FTIR spectrum of purified anthocyanins from BP, WB, and BB was recorded ranging from 400–4000 cm^{-1} (ESI Fig. 3†). The vibrational bands at 600 to 1000 cm^{-1} correspond to the aromatic rings. This region is known as a fingerprint region as it is majorly associated with complex vibrational changes in molecules.[37] The absorption band at 1500 to 2000 cm^{-1} confirms the presence of a benzene ring (C=C/C=N/C=O) in the sample. The region at around 3600 to 3200 cm^{-1} corresponds to H-bonds and the broad band at around 3000 to 2800 cm^{-1} represents C–H/O–H/N–H groups. Thus, FTIR spectral analysis of anthocyanins exhibited the presence of O–H, C=O, C=C, and C–O–C which are the characteristic functional groups of anthocyanins.[38] Furthermore, absorbance at 1018 cm^{-1} and 1246 cm^{-1} corresponds to the stretching vibration of the C–O–C esters and the stretching of pyran rings, respectively. Whereas, absorbance bands at 1423, 1647, and 1707 cm^{-1} are ascribed to C–O deformation of phenols, C=C, and C=O groups for aromatic rings, respectively. The absorbance band at around 1600 cm^{-1} represents the skeletal stretching vibration of aromatic rings A and B of anthocyanins and =C–O–C of the C ring of flavones. The bands at around 1514, 1462, 1246, and 1018 cm^{-1} correspond to the stretching vibration of the =C–O–C group present in the aromatic ring of flavonoids. In addition, the bands at 804 cm^{-1} and 742 cm^{-1} present vibration of anthocyanins.[39] Additionally, the FTIR spectrum of kraft lignin was also acquired. Notably, the peaks at 1217, 1340, 1420, 1580, 2950, and 3480 cm^{-1} represent C=O stretching and C=C stretching vibrations in aromatic rings of lignin corresponding to CH and OH functional groups.[17] Interestingly, FTIR spectra of developed nanoparticles BP@ALNPs, WB@ALNPs, and BB@ALNPs showed characteristic peaks of purified anthocyanins along with lignin, which confirms the synthesis of A-LNPs.

Stability study of A-LNPs

The stability of bare LNPs, BP@ALNPs, BB@ALNPs, and WB@ALNPs was explored at room temperature for 4 weeks under natural light (daily exposure for 16 h) using DLS. During storage, insignificant variations were observed in particle size, PDI, and zeta potential (ESI Fig. 4†) for up to 28 days. Thus, synthesized A-LNPs were stable for a long time at room temperature and no aggregation was observed. A previous study has also reported high stability in the case of pyranoanthocyanin-LNPs and portisin-LNPs but they mentioned an increase in the size of bare LNPs.[31]

The phenolic hydroxyl and carboxyl groups available on the surface of LNPs are responsible for their negative charge. This promotes the formation of electrical double layers which stabilizes nanoparticle dispersion through electrical double-layer repulsion.[35,36] As observed in ESI Fig. 4,† the average zeta potential of A-LNPs remains the same with values of around −35 mV after 28 days of storage at room temperature. These observations confirm the high stability and efficient application of synthesized nanoparticles for long-term use as an active ingredient in packaging materials.

Antioxidant activity of A-LNPs

Furthermore, A-LNPs were explored for their antioxidant activity by employing ABTS and DPPH assays. Exploration of the antioxidant activity by employing a single method does not provide a comprehensive understanding of the antioxidant activity of a sample due to the lack of specificity and sensitivity of a particular assay.[40] Thus, ABTS and DPPH assays were employed to explore the antioxidative potential of purified anthocyanins and A-LNPs. The principle of the ABTS method is based on the discoloration of ABTS+ by reducing it with antioxidative compounds present in the samples. In the case of the DPPH assay, discoloration of the violet-colored DPPH reagent indicates the transformation of a DPPH free radical into the reduced DPPH-H form due to the antioxidants available in the sample.[41] As shown in ESI Table 4.† purified anthocyanins from various sources presented a potent antioxidant activity of 60.98–62.30% and 69.43–72.24% as assessed by ABTS and DPPH assays,

respectively. These findings were supported by previous authors and WB, BB, and BP were mentioned to exhibit high antioxidant activities.[42–44] However, variations in antioxidant activity compared to previous studies may be attributed to different geographical locations and ripening levels of the samples.[2] Moreover, bare LNPs were also observed to be potent antioxidants with 64.03% and 67.68% antioxidant activity as assessed with ABTS assay and DPPH assay, respectively. The presence of a large number of phenolic groups is responsible for the potent antioxidant activity of lignin.[17,18] However, it is interesting to observe that A-LNPs present significantly enhanced antioxidant activity compared to purified anthocyanins and bare LNPs. Among all A-LNPs, WB@ALNPs presented the highest antioxidant activity followed by BP@ALNPs and BB@ALNPs. Previously, beta-carotene nanoencapsulated in alkali lignin-based nanofibers and BP phenolic compounds nanoencapsulated in pectin–whey protein isolate also presented enhanced antioxidant activity as assessed by the DPPH and ABTS assays.[45,46] The enhanced antioxidant activity of encapsulated bioactive compounds was reported to be associated with the increase in the surface area of resultant nanoparticles due to their small size obtained through nanoencapsulation. This results in a greater number of chemical interactions, higher stabilization of active compounds, and enhanced dispersibility, bioaccessibility, and bioavailability of the nanoencapsulated compounds. This in turn results in higher antioxidant activity of nanoencapsulated bioactive compounds.[46]

Antimicrobial activity

Based on the literature[17,18] and findings of antioxidant activity in the present study, synthesized A-LNPs are also expected to exhibit potent antibacterial activity. Thus, the antibacterial activity of A-LNPs was explored against the most prevalent foodborne pathogen *S. aureus* using the spread plate method. *S. aureus* is the major cause of foodborne diseases globally.[47] Thus, the antibacterial activity of synthesized A-LNPs against *S. aureus* is of great significance. As shown in Fig. 2, it was observed that lignin and purified anthocyanins exhibit potent antibacterial activity against *S. aureus*. However, A-LNPs presented significantly enhanced antibacterial activity compared to bare LNPs and purified anthocyanins. Furthermore, the IC_{50} of A-LNPs against *S. aureus* (15.82–17.56 μg mL^{-1}) was significantly lower compared to that of purified anthocyanins (21.18–32.22 μg mL^{-1}) and bare LNPs (60.22 μg mL^{-1}) as shown in ESI Table 5.† Among all A-LNPs, BB@ALNPs exhibited the lowest IC_{50} value of 15.82 μg mL^{-1}. Similar findings were also reported in previous studies where LNPs were reported to exhibit antibacterial activity against different bacteria by disrupting their cell membrane and releasing their cytoplasmic content.[17] Thus, BB@ALNPs can be efficiently employed as an active agent to develop antimicrobial packaging materials for enhancing the shelf life of perishable food materials.

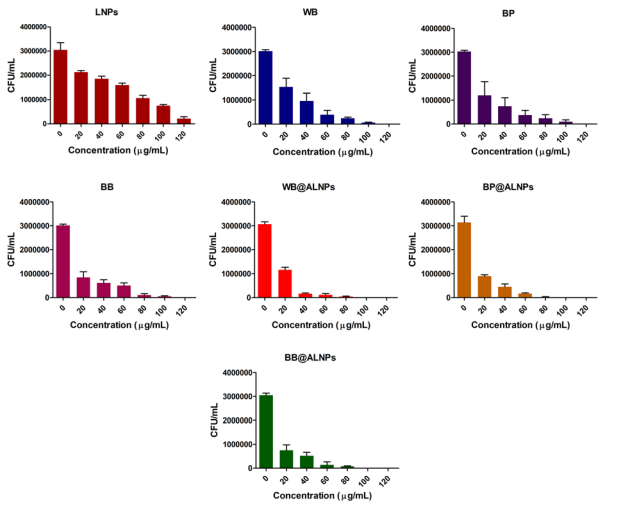

Fig. 2 Antimicrobial activity of bare LNPs, purified anthocyanins, and A-LNPs against *S. aureus*.

Development and characterization of PVA–PEG-A-LNPs packaging films

Color. As shown in Fig. 3(a–h), the PVA–PEG-A-LNPs-based packaging films were developed using BB@ALNPs at different concentrations (1–20%). The bare PVA–PEG-based film was transparent whereas packaging films containing BB@ALNPs exhibited brownish color due to the presence of lignin. The color of films was increased with increased concentration of BB@ALNPs. Similar results were also reported in lignin-

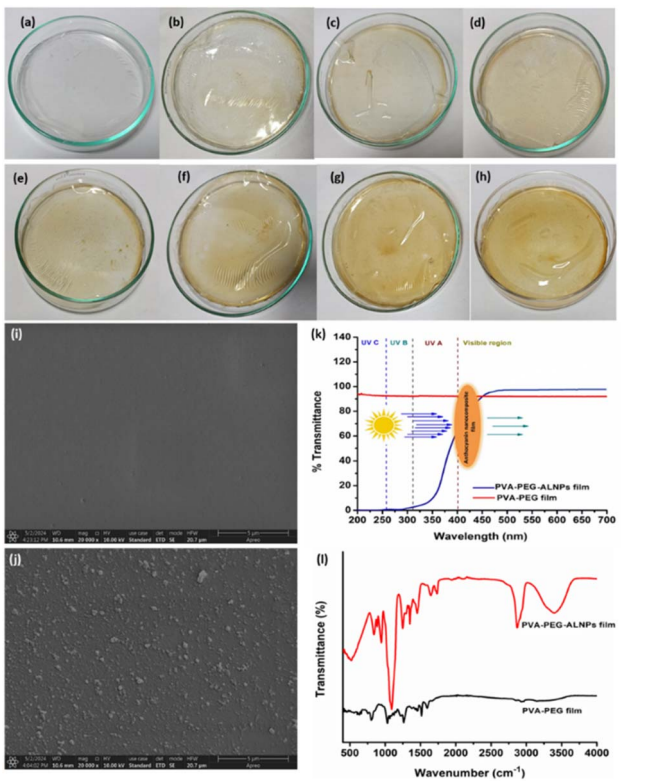

Fig. 3 PVA–PEG-A-LNPs-based packaging films containing (a) no ALNPs, and (b) 1%, (c) 3%, (d) 5%, (e) 7%, (f) 10%, (g) 15%, and (h) 20% BB@ALNPs, and characterization of packaging films: (i) SEM of a bare PVA–PEG film, (j) SEM of PVA–PEG_BB@ALNPs, (k) UV blocking properties, and (l) FTIR spectrum of films.

containing cellulose nanopaper and pectin-nanolignin composite films.[48,49]

Mechanical properties. As described in ESI Table 6,† the tensile strength of the bare PVA–PEG film was 1.50 MPa, whereas a significant increase in the tensile strength was observed in PVA–PEG-A-LNPs-based packaging films (1.50–8.79 MPa). Similar results were also reported while developing PVA–PEG-based lignin nanocomposite films.[19] The maximum tensile strength was observed in the case of PVA–PEG_15%BB@ALNPs (8.79 kg m^{-2}), which further decreased with an increase in the concentration of BB@ALNPs to 20%. This observation is in agreement with previous studies where lignin-nanosphere-based PVA films and nanolignin-based poly (lactic acid)-poly (ε-caprolactone) films showed an increase in tensile strength with an increase in LNPs and a significant decrease in tensile strength with a further increase in the LNPs.[50,51] This increase in the tensile strength is attributed to the strong hydrogen bonds formed between LNPs and PVA which results in a high level of interfacial adhesion. In addition, LNPs also act as a cross-linker in PVA that restricts the motion of the PVA molecular chain and improves the mechanical properties of packaging films.[50] Furthermore, the bare PVA–PEG-based film presented brittle behavior with the lowest elongation at break value (13.60%) and PVA–PEG_15%BB@ALNPs-based films exhibited the highest value for elongation at break (47.52%). Moreover, the addition of 20% BB@ALNPs reduces the elongation at break along with the tensile strength because the addition of a high amount of LNPs in films generates microphase separation.[50] In addition, the WVTR of PVA–PEG_15%BB@ALNPs-based films was also less compared to that of bare films. The higher WVTR reduces the shelf-life of packaged food.[23] Thus, based on the findings of tensile strength, elongation at break, and WVTR, for further analysis, PVA–PEG_15%BB@ALNPs-based films were explored and compared with bare PVA–PEG-based films. Furthermore, as shown in ESI Table 7,† a migration test of PEG_15%BB@ALNPs-based films was also conducted with water, 30% acetic acid, 50% ethanol, and *n*-heptane to explore the suitability of the novel synthesized film for food packaging. In case of all samples, the results are significant. Also in the case of *n*-pentane (as observed at 1.80 mg kg^{-1}), and for below the established limit (60 mg kg^{-1}). Furthermore, film production provides additional protection against migration in several kinds of circumstances. For example, in the case of 3% acetic acid, the PVA–PEG film without active chemicals exhibits migration values up to 5 times greater than those of the active film samples. Additionally, the PVA–PEG-15%BB@ALNPs-based film showed 8 times greater than the reported migration limit (60 mg kg^{-1}). Therefore, the safety-in-use hypothesis already inferred from a specific migration research is supported by overall migration testing.

The uniform thickness for bare PVA–PEG and PVA–PEG_15% BB@ALNPs-based films was 0.059 and 0.068 mm, respectively. These findings agreed with a previous study where PVA–PEG-based films were developed using different concentrations of lignin and copper oxide nanoparticles.[19]

Morphological and FTIR spectral analysis. The SEM analysis of bare PVA–PEG presented smooth morphology (Fig. 3(i)), whereas the PVA–PEG_15%BB@ALNPs film presented a rough surface due to the presence of well-dispersed ALNPs (Fig. 3(j)). These observations are in agreement with previous studies on nanolignin-based PVA films.[19,50] As observed in Fig. 3(l), FTIR spectra of PVA–PEG present a vibration band at 2919 cm^{-1} corresponding to the stretching vibration of the CH_2 group, and a broad band at around 3300 cm^{-1} presenting the stretching vibrations of OH group. The bands at 1679 cm^{-1} correspond to the existence of vinyl alcohol and bands at 1736 and 1583 cm^{-1} correspond to the C=O carbonyl group of the acetate group. Furthermore, bands at 1470, 1350, 1118, and 956 cm^{-1} represent a symmetrical CH_2, stretching vibrations of mixed CH– and OH– bending, and C–C stretching of the *trans*-arrangement of the planar zigzag syndiotactic structure of PVA, respectively.[52] However, in the case of PVA–PEG_BB@ALNPs films, additional peaks representing anthocyanins (3000 to 2800 cm^{-1}, 1514, 1462, 1246, and 1018 cm^{-1}) and lignin (1217, 1340, 1420, 1580, 2950, and 3480 cm^{-1}) were also observed.[17,38,39] This confirms the successful synthesis of PVA–PEG_15%BB@ALNPs films.

UV blocking and fluorescence properties. It is well known that UV light degrades food quality and significantly reduces the shelf life through photo-oxidation.[48] Thus, UV-blocking properties in packaging materials are highly appreciated. Furthermore, UV-vis analysis of PVA–PEG_15%BB@ALNPs films revealed excellent UV-blocking properties with 0% transmittance in UVC and UVB regions, whereas bare PVA–PEG presented around 93.5% transmittance as shown in Fig. 3 (k). The UV-blocking properties of PVA–PEG_15%BB@ALNPs films were attributed to the well-known UV shielding capability of lignin.[17] Similar UV-blocking properties were also observed in the case of previously developed PVA-nanolignin, pectin-nanolignin, and PVA-lignin nanosphere-based composite films.[48,50,53] The presence of specific phenolic hydroxyl groups and chromophores in the LNP structure is responsible for the UV blocking properties of PVA–PEG_15%BB@ALNPs films.[19,48] As shown in ESI Fig. 5,† the PVA–PEG_15%BB@ALNPs film showed significant fluorescence which is attributed to the presence of LNPs in it, whereas bare PVA–PEG films are not fluorescent.

Postharvest quality measurement of tomatoes packaged with PVA–PEG-A-LNPs films

Furthermore, the quality parameters of tomatoes packaged with PVA–PEG_BB@ALNPs films and PVA–PEG films were explored and compared with those of unpackaged tomatoes to elucidate the impact of PVA–PEG_BB@ALNPs films on the shelf life of tomatoes. As shown in ESI Table 8,† the weight loss of samples was increased as a function of storage time. The highest weight loss was observed in the control group and the least weight loss was found in tomatoes packaged with PVA–PEG_BB@ALNPs films. Similar results were also observed in a previous study where application of an edible multilayer coating has reduced the weight loss in cherry tomatoes.[25] Weight loss results in textural changes and surface shrinkage of tomatoes.[54] As observed in Fig. 4, significant textural changes and shrinkage were observed in the control group compared to slight

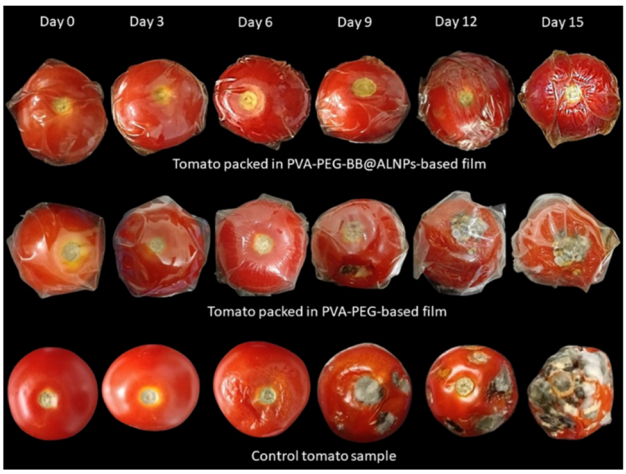

Fig. 4 Visual examination of the gradual quality change of tomatoes during 15 days of storage.

shrinkage or textural variation on tomatoes packaged with the PVA–PEG_BB@ALNPs film on the 15th day. The reduced weight loss in packaged samples revealed that PVA–PEG-based films act as a semi-permeable barrier against solute movement, gases, and moisture.[55]

Firmness is an important textural parameter that significantly affects consumers' acceptability towards a food. It was interesting to observe that tomatoes packaged with the PVA–PEG_BB@ALNPs film showed maximum resistance against firmness loss, whereas the PVA–PEG group showed slight resistance toward weight loss (ESI Table 8†). These findings agree with previous research where tomato samples coated with an edible nanoemulsion containing carboxymethyl cellulose and cardamom oil exhibited resilience to loss of firmness.[54] However, maximum firmness loss was observed in the control group. In the case of color values (L^*, a^*, and b^*), the least variations were observed in tomatoes packaged with the PVA–PEG_BB@ALNPs film, and maximum variations were found in the control group. This observation was in agreement with a previous study where cherry tomatoes packed with poly(3-hydroxybutyrate)/grapeseed oil/MgO nanocomposite films presented the least change in color values whereas color of control samples varied significantly during storage.[56] The pH of tomatoes was increased with an increase in the maturation and storage time. Furthermore, the increase in pH is proportional to the decrease in the TA values of the samples, which represents a decrease in acid content in tomatoes with maturity.[57] Thus, according to the findings of the present study, PVA–PEG_BB@ALNPs-based packaging significantly delayed the ripening stage of tomatoes compared to PVA–PEG packaging and the control group. In addition, a gradual increase in the TSS values was also observed in tomatoes of all groups with an increase in the storage time. However, the TSS values in the control group were significantly higher than those in the PVA–PEG and PVA–PEG_BB@ALNPs packaged group. Whereas, the least increase in TSS values was observed in the PVA–PEG_BB@ALNPs packaged group which is attributed to slow respiration in this group, which in turn delayed the utilization and synthesis of metabolites.[55] Similar observations were also reported in the case of tomato samples packaged with chitosan–titanium dioxide nanocomposite films.[58] Thus, tomatoes packaged with PVA–PEG_BB@ALNPs films present high resistance towards quality deterioration during 15 days of storage at room temperature compared to tomatoes packaged with the PVA–PEG film and the control group.

Conclusions

In the present study, anthocyanins were extracted from agro-waste, purified, and then nanoencapsulated using lignin (A-LNPs). The successful synthesis of A-LNPs was confirmed by employing DLS, SEM, TEM, and FTIR analysis. The encapsulation of anthocyanin using lignin leads to enhanced stability, antioxidant activity, and antimicrobial activity of A-LNPs compared to purified anthocyanins and lignin. Overall, BB resulted in the highest TAC (194.45 mg per kg WB) and good encapsulation efficiency (92.32%) along with potent antioxidant (73.32–79.56%) and antibacterial activity (15.82 μg mL^{-1}) against *S. aureus*. Furthermore, 15% BB@ALNPs was used as an active ingredient for developing PVA–PEG-based packaging films. These films exhibited excellent tensile strength, UV-blocking, and fluorescence properties. These films were also characterized by employing SEM and FTIR spectroscopy. Furthermore, tomatoes were packaged with PVA–PEG_15% BB@ALNPs and PVA–PEG-based films. The samples packaged with PVA–PEG_15%BB@ALNPs films presented high resistance towards quality deterioration compared to tomatoes packaged with PVA–PEG films and control samples during 15 days of storage at room temperature. In the future, the antimicrobial potential of PVA–PEG_15%BB@ALNPs films can be explored against various food-borne pathogens. In addition, PVA–PEG_15%BB@ALNPs films can also be employed as an intelligent packaging or biosensor to monitor the shelf life of various perishable food products based on the fluorescence properties of PVA–PEG_15%BB@ALNPs films. Overall, the present findings will contribute significantly towards the sustainable development goals set by the United Nations and the Government of India's vision to be among the top five global bio-manufacturing hubs by 2025.

Data availability

The data supporting this article have been included as part of the ESI.†

Author contributions

Maninder Meenu: conceptualization, data curation, methodology, investigation, writing – original draft, visualization, supervision, project administration. Anil Kumar Pujari: investigation, methodology. Seema Kirar: review & editing. Mansi: data curation, methodology, investigation. Aniket Thakur: data curation, methodology, investigation. Monika Garg: methodology, project administration, supervision, review & editing.

Jayeeta Bhaumik: conceptualization, investigation, supervision, project administration, review & editing.

Conflicts of interest

A patent has been applied based on this work with Indian patent application no 202311083795. The authors declare that they have no known competing financial interests or personal relationships that could have appeared to influence the work reported in this paper.

Acknowledgements

The authors would like to acknowledge the Department of Biotechnology (DBT), Govt. of India, for funding and infrastructural support. This work was supported by the M. K. Bhan Young Researcher Fellowship; Department of Biotechnology, New Delhi, India. J. B. thanks the Department of Biotechnology, Govt. of India, for funding under the lignin valorization flagship project. S. K. appreciates the Department of Science and Technology (DST) for a Women Scientist-A (WOS-A) fellowship. A. K. P. is grateful to CIAB for a senior research fellowship. The authors would also like to acknowledge the NABI and CIAB Mohali for providing the instrumentation facilities.

References

1 F. Guo and F. Shahidi, *Trends Food Sci. Technol.*, 2024, **143**, 104219.
2 M. Meenu, V. Bansal, S. Rana, N. Sharma, V. Kumar, V. Arora and M. Garg, *Sustainable Chem. Pharm.*, 2023, **34**, 101168.
3 Y. Cheng, J. Liu, L. Li, J. Ren, J. Lu and F. Luo, *Food Chem.: X*, 2023, **20**, 100983.
4 N. Oladzadabbasabadi, A. Mohammadi Nafchi, M. Ghasemlou, F. Ariffin, Z. Singh and A. A. Al-Hassan, *Food Packag. Shelf Life*, 2022, **33**, 100872.
5 T. K. O. Rosales and J. P. Fabi, *Colloids Surf., B*, 2022, **218**, 112707.
6 H. Zhang, C. Jia, Y. Xiao, J. Zhang, J. Yu, X. Li, N. Hamid and A. Sun, *Food Chem.*, 2024, **439**, 138150.
7 Y. Qin, Y. Liu, L. Yuan, H. Yong and J. Liu, *Food Hydrocoll.*, 2019, **96**, 102–111.
8 A. A. Escobar-Puentes, A. García-Gurrola, S. Rincón, A. Zepeda and F. Martínez-Bustos, *Carbohydr. Polym.*, 2020, **250**, 116972.
9 L. Yao, J. Xu, L. Zhang, L. Liu and L. Zhang, *Food Hydrocoll.*, 2021, **118**, 106741.
10 T. K. O. Rosales, M. Pessoa da Silva, F. R. Lourenço, N. M. A. Hassimotto and J. P. Fabi, *Food Hydrocoll.*, 2021, **114**, 106563.
11 R. Rashid, S. M. Wani, S. Manzoor, F. A. Masoodi and A. Altaf, *Food Biosci.*, 2022, **50**, 102135.
12 A. Dinari, M. Abdollahi and M. Sadeghizadeh, *Sci. Rep.*, 2021, **11**(1), 1–16.
13 F. Zikeli, V. Vinciguerra, S. Sennato, G. Scarascia Mugnozza and M. Romagnoli, *ACS Omega*, 2020, **5**, 358–368.
14 S. Jaiswal, M. M. Anjum, S. Thakur, P. Pandey, D. K. Arya, A. Kumar, A. S. Kaushik and P. S. Rajinikanth, *J. Drug Deliv. Sci. Technol.*, 2023, **89**, 105076.
15 H. jia Xiang, A. ling Zhong, H. Wang, L. Xiao, T. ren Deng, T. gen Hu and P. Wen, *Int. J. Biol. Macromol.*, 2022, **218**, 739–750.
16 P. Araújo, A. Costa, I. Fernandes, N. Mateus, V. de Freitas, B. Sarmento and J. Oliveira, *Dyes Pigm.*, 2019, **166**, 367–374.
17 S. Paul, N. S. Thakur, S. Chandna, Y. N. Reddy and J. Bhaumik, *J. Mater. Chem. B*, 2021, **9**, 1592–1603.
18 R. Kaur, N. S. Thakur, S. Chandna and J. Bhaumik, *ACS Sustain. Chem. Eng.*, 2021, **9**, 11223–11237.
19 S. Kirar, D. Mohne, M. Singh, V. Sagar, A. Bhise, S. Goswami and J. Bhaumik, *Sustainable Mater. Technol.*, 2024, **40**, e00864.
20 A. Sharma, M. Yadav, N. Sharma, A. Kumari, S. Kaur, M. Meenu and M. Garg, *Food Res. Int.*, 2022, **161**, 111833.
21 R. P. Hutabarat, Y. D. Xiao, H. Wu, J. Wang, D. J. Li and W. Y. Huang, *J. Food Qual.*, 2019, **2019**, 1–10.
22 N. Solarte, M. J. Cejudo-Bastante, N. Hurtado and F. J. Heredia, *Int. J. Food Sci. Technol.*, 2022, **57**, 2416–2423.
23 E. L. Hanry and N. Surugau, *J. Appl. Phycol.*, 2024, **36**, 917–934.
24 I. S. Arvanitoyannis and L. Bosnea, *Crit. Rev. Food Sci. Nutr.*, 2004, **44**, 63–76.
25 D. A. Carrillo-Lomelí, M. A. Cerqueira, V. Moo-Huchin, A. I. Bourbon, V. G. L. Souza, A. Lestido-Cardama, L. M. Pastrana, Y. M. Ochoa-Fuentes, F. D. Hernández-Castillo, J. Á. Villarreal-Quintanilla and D. Jasso de Rodríguez, *Sci. Hortic.*, 2024, **332**, 113224.
26 A. J. Hu, S. T. Hao, J. Zheng, L. Chen and P. P. Sun, *J. AOAC Int.*, 2021, **104**, 811–817.
27 W. Liao, W. Badri, E. Dumas, S. Ghnimi, A. Elaissari, R. Saurel and A. Gharsallaoui, *Appl. Sci.*, 2021, **11**, 5778.
28 R. Esfahani, S. M. Jafari, A. Jafarpour and D. Dehnad, *Food Hydrocoll.*, 2019, **90**, 291–298.
29 M. A. Çakır, N. C. Icyer and F. Tornuk, *Int. J. Biol. Macromol.*, 2020, **151**, 230–238.
30 L. Dai, R. Liu, L. Q. Hu, Z. F. Zou and C. L. Si, *ACS Sustain. Chem. Eng.*, 2017, **5**, 8241–8249.
31 P. Araújo, A. Costa, I. Fernandes, N. Mateus, V. de Freitas, B. Sarmento and J. Oliveira, *Dyes Pigm.*, 2019, **166**, 367–374.
32 D. D. Herrera-Balandrano, Z. Chai, T. Beta, J. Feng and W. Huang, *Trends Food Sci. Technol.*, 2021, **118**, 808–821.
33 N. R. R. do Nascimento-Silva, R. P. Bastos and F. A. da Silva, *J. Food Compos. Anal.*, 2022, **109**, 104491.
34 A. Kumari, S. Kaur, N. Sharma, J. Kaur, M. Krishania, V. Tiwari and M. Garg, *J. Cereal. Sci.*, 2022, **108**, 103560.
35 P. Figueiredo, K. Lintinen, A. Kiriazis, V. Hynninen, Z. Liu, T. Bauleth-Ramos, A. Rahikkala, A. Correia, T. Kohout, B. Sarmento, J. Yli-Kauhaluoma, J. Hirvonen, O. Ikkala, M. A. Kostiainen and H. A. Santos, *Biomaterials*, 2017, **121**, 97–108.
36 M. Lievonen, J. J. Valle-Delgado, M. L. Mattinen, E. L. Hult, K. Lintinen, M. A. Kostiainen, A. Paananen, G. R. Szilvay, H. Setälä and M. Österberg, *Green Chem.*, 2016, **18**, 1416–1422.

37 M. Meenu and B. Xu, *Food Chem.*, 2019, **289**, 545–557.
38 B. Bhushan, B. Bibwe, A. Pal, M. K. Mahawar, M. C. Dagla, Y. KR, B. S. Jat, P. Kumar, S. K. Aggarwal, A. Singh and D. P. Chaudhary, *Appl. Food Res.*, 2023, **3**, 100282.
39 R. Różyło, M. Szymańska-Chargot, U. Gawlik-Dziki and D. Dziki, *Food Chem.*, 2021, **346**, 128889.
40 Y. Zhang, M. Meenu, H. Yu and B. Xu, *Foods*, 2020, **9**, 438.
41 J. Zheng, X. Yu, M. Maninder and B. Xu, *Int. J. Food Prop.*, 2018, **21**, 1524–1540.
42 M. D. M. Sousa, R. M. T. de Lima, A. de Lima, A. C. Reis, A. A. de, C. M. Cavalcante, J. A. G. Sattler, L. B. de Almeida-Muradian, J. D. S. Lima Neto, R. S. dos, R. Moreira-Araujo and N. D. N. Nogueira, *Food Chem.*, 2021, **363**, 130353.
43 T. O. Adedokun, A. Matemu, O. Höglinger, E. Mlyuka and A. Adedeji, *Heliyon*, 2022, **8**, e09340.
44 A. Liu, H. Li, W. Xu, L. Zhu, S. Ye, T. Li, J. Li, S. Chang and C. Xie, *LWT*, 2024, **213**, 117049.
45 H. jia Xiang, A. ling Zhong, H. Wang, L. Xiao, T. ren Deng, T. gen Hu and P. Wen, *Int. J. Biol. Macromol.*, 2022, **218**, 739–750.
46 J. A. Barbosa dos Santos, C. F. Assis, C. F. Soares Aragao, M. dos Santos Lima, T. S. Passos and J. K. da Silva-Maia, *Heliyon*, 2024, **10**, e36973.
47 H. O. Khalifa, M. A. A. Abdelhamid, A. Oreiby, M. Y. Ibrahim Mohamed, H. Ramadan, A. Elfadadny, S. P. Pack, H. S. Yoo and I. Habib, *J. Agric. Food Res.*, 2025, **19**, 101606.
48 S. Zhang, X. Cheng, Q. Fu, Y. Li, P. Wu, Y. Qiao, J. Yan, L. Si, G. I. N. Waterhouse, H. Li and S. Ai, *Food Hydrocoll.*, 2023, **143**, 108783.
49 Y. Zhang, Y. Wei, Y. Qian, M. Zhang, P. Zhu and G. Chen, *ACS Sustain. Chem. Eng.*, 2020, **8**, 17033–17041.
50 F. Xiong, Y. Wu, G. Li, Y. Han and F. Chu, *Ind. Eng. Chem. Res.*, 2018, **57**, 1207–1212.
51 W. Yang, G. Qi, H. Ding, P. Xu, W. Dong, X. Zhu, T. Zheng and P. Ma, *Compos. Commun.*, 2020, **22**, 100497.
52 Z. K. Heiba, M. Bakr Mohamed and S. I. Ahmed, *Alex. Eng. J.*, 2022, **61**, 3375–3383.
53 W. Yang, H. Ding, G. Qi, C. Li, P. Xu, T. Zheng, X. Zhu, J. M. Kenny, D. Puglia and P. Ma, *React. Funct. Polym.*, 2021, **162**, 104873.
54 S. K. Das, K. Vishakha, S. Das, D. Chakraborty and A. Ganguli, *Biocatal. Agric. Biotechnol.*, 2022, **42**, 102369.
55 A. Nawab, F. Alam and A. Hasnain, *Int. J. Biol. Macromol.*, 2017, **103**, 581–586.
56 S. Venu Gopala Kumari, K. Pakshirajan and G. Pugazhenthi, *Sustainable Chem. Pharm.*, 2024, **41**, 101681.
57 E. de J. Salas-Méndez, A. Vicente, A. C. Pinheiro, L. F. Ballesteros, P. Silva, R. Rodríguez-García, F. D. Hernández-Castillo, M. de, L. V. Díaz-Jiménez, M. L. Flores-López, J. Á. Villarreal-Quintanilla, F. M. Peña-Ramos, D. A. Carrillo-Lomelí and D. Jasso de Rodríguez, *Postharvest Biol. Technol.*, 2019, **150**, 19–27.
58 P. Kaewklin, U. Siripatrawan, A. Suwanagul and Y. S. Lee, *Int. J. Biol. Macromol.*, 2018, **112**, 523–529.